Molecular Crystals and Liquid Crystals
Publication details, including instructions for authors and subscription information:
http://www.informaworld.com/smpp/title~content=t713644168

Long Pitch Orthoconic Antiferroelectric Binary Mixture for Display Applications

W. Piecek[a]; P. Perkowski[a]; Z. Raszewski[a]; P. Morawiak[a]; M. Żurowska[b]; R. Dąbrowski[b]; K. Czupryński[b]
[a] Institute of Applied Physics, MUT, Warszawa, Poland [b] Institute of Chemistry, MUT, Warszawa, Poland

First published on: 13 July 2010

To cite this Article Piecek, W. , Perkowski, P. , Raszewski, Z. , Morawiak, P. , Żurowska, M. , Dąbrowski, R. and Czupryński, K.(2010) 'Long Pitch Orthoconic Antiferroelectric Binary Mixture for Display Applications', Molecular Crystals and Liquid Crystals, 525: 1, 140 — 152
To link to this Article: DOI: 10.1080/15421401003796223
URL: http://dx.doi.org/10.1080/15421401003796223

Mol. Cryst. Liq. Cryst., Vol. 525: pp. 140–152, 2010

ISSN: 1542-1406 print/1563-5287 online
DOI: 10.1080/15421401003796223

Taylor & Francis
Taylor & Francis Group

Long Pitch Orthoconic Antiferroelectric Binary Mixture for Display Applications

W. PIECEK,[1] P. PERKOWSKI,[1] Z. RASZEWSKI,[1] P. MORAWIAK,[1] M. ŻUROWSKA,[2] R. DĄBROWSKI,[2] AND K. CZUPRYŃSKI[2]

[1]Institute of Applied Physics, MUT, Warszawa, Poland
[2]Institute of Chemistry, MUT, Warszawa, Poland

Orthoconic Antiferroelectric Liq. Cryst. (OAFLC) have been extensively studied due to their unique electrooptical properties [1,2]. Practical implementation of this kind of liquid crystalline medium experiences many obstacles including a number of parasitic effects deteriorating the electrooptical performance. In search for working OAFLC a mixture with the helical pitch longer than the typical cell gap was formulated. Using this mixture near perfect optical uniformity and excellent dark state at the zero electric field applied was obtained. The physical and structural properties of mixture are presented and their parameters are discussed. The electrooptical performance is presented and discussed.

Keywords Helical pitch; high tilted smectic; orthoconic antiferroelectric smectic liquid crystals

Introduction

Antiferroelectric liquid crystals (AFLC) at surface stabilized geometry (SSAFLC) have been extensively studied due to their physical properties offering unique electrooptical performance [1–6]. AFLC's intrinsic non-linearity promotes a utilization of the relatively simple passive symmetrical multiplexing method for full scale displays [7]. This promises a good resistance to ionic memory effect and makes the induction of the gray scale realistic [8]. However, the practical implementation of those structures is hampered by two main obstacles: i) rather poor optical uniformity of the structure obtained within a standard cell of thickness approximately 2 [μm] [7,9], and ii) so called "pretransitional effect," which is a gradual degradation of the black state upon voltage increasing [10,11]. Both effects deteriorate the contrast of the optical reproduction needed by contemporary displays.

The first problem seems to be eliminated by utilization of the high tilted AFLCs where the molecular tilt reaches the optimal value of 45°. Such ALFC are called orthoconic antiferroelectric liquid crystals (OAFLC) [2]. OAFLC at a surface

Address correspondence to W. Piecek, Ph.D., Eng., Adiunkt, Institute of Applied Physics, Department of New Technologies and Chemistry, Military University of Technology, Kaliskiego 2 St., 00-908 Warszawa, Poland. Tel.: + 48 22 683 9731; Fax: + 48 22 683 9262; E-mail: wpiecek@wat.edu.pl

stabilized bookshelf structure (usually obtained within cells with 1.5 [μm] cell gap) provide excellent dark state at zero electric field applied.

Besides the pure soft mode electroclinic behavior, the pretransitional effect is ascribed to the collective movement of molecules around the cone. This effect occurs when the remains of molecular helix exist within the structure. This is a common case when the helix is usually not completely unwound upon surface action in 1.5 [μm] cells [12]. This explanation can be supported by observations which prove that a significant higher contrast can be obtained in reflective mode, utilizing cells with cell gap 0.8 [μm] only. So, in search for the OAFLC material free from the light leakage upon low electric field regime the effort was done to find a method for the complete helix unwinding within typical 1.5 [μm] cell.

The application of strong boundary conditions for the complete helix unwinding of typical OAFLCs often leads to the elimination of the anticlinic structure in favor of synclinic one. Moreover, strong boundary conditions may induce the threshold less switching [13]. So, the OAFLC with the molecular pitch significantly longer than the cell gap was searched as an alternative solution for obtaining helixless bookshelf structure within 1.5 [μm] cells. This is assumed as a method for eliminating of the pretransitional effect.

Since the usually obtained anticlinic materials form macroscopic helix with the helical pitch of about 1 [μm], we assume that for obtaining helixless bookshelf structure within typical 1.5 [μm] cells, an OAFLC with the helical pitch exceeding 3 [μm] is needed. Detailed molecular properties inducing long helical pitch at the SmC^*_A phase still are unraveled. The motivation of this work was to test whether the involving the molecular incompatibility within a single molecular layer is able to induce the elongation of the molecular pitch. The search for homologues components for the working mixture was started from compounds exhibiting the longest value of the helical pitch. The binary, equimolar mixture was formulated using such two homologous compounds. In this study we present structural and physical properties of binary mixture and we discuss its parameters in context of the molecular properties of mixture components and physical properties of the anticlinic phases formed by them.

Experiment

A two homostructural compounds (see Fig. 1) with biphenyl benzoate based molecular rigid core, partially fluorinated alkoxyalkoxy terminal chain [4,14] and 1-methylheptyloxy chiral centre (abbreviated here CM1 [15] and CM2 [16]) were chosen for investigations (see Fig. 1 and Table 1). The near equimolar mixture, abbreviated W1000, was prepared using 0.475% (mole fraction) of CM1 compound and 0.525% (mole fraction) of compound CM2. The structural difference between compounds is the length of the hydrocarbon spacer and the position of the fluorine atom substituted at the benzene ring within molecular rigid core. Mentioned compounds were selected because they exhibit the longest helical pitch at the anticlinic phase (see Fig. 2) within the homologues series [15,17]. We have chosen these compounds for the working OAFLC mixture formulation despite the fact that both of them did not exhibit desired three stable switching while typical 1.5 [μm] cells are used. Compound CM1 exhibits V-shape switching while compound CM2 exhibits W – shape switching. The synthesis of high optical purity antiferroelectric compounds was described elsewhere [15,16,18].

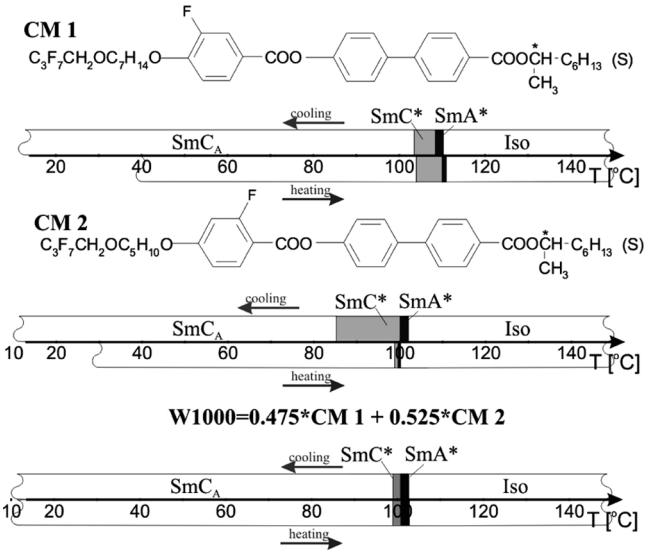

Figure 1. The template structure of compounds CM1 and CM2 and the mesogenic behavior of those compounds and the mixture W1000.

The mesogenic behavior was studied by using of DSC "Setaram" 141 micro calorimeter. Phase transitions as well as their enthalpies were detected upon subsequent heating and cooling cycles at the rate of 2 [K/min]. These studies were combined with the microscopic observations using Biolar PI polarizing microscope equipped with the Instec hot stage controlled by the Instec STC200 driving unit and PC. Results are presented in Table 1 and in Figure 1. Used compounds have low melting point (see Table 1) and low melting enthalpy (ibid). Such parameters enabled us to formulate a mixture exhibiting a broad temperature range of anticlinic phase with a saturated value of the tilt angle over 40°. As to follow correlation of molecular properties with physical properties of the orthoconic SmC^*_A phase, the molecular modeling was done using HyperChem 7.5 molecular modeling system. The aim of this task was to obtain the most stable molecular conformation, molecular dimensions, the overall molecular dipole moment and the dipole moment components within assumed frame of coordinates (see Table 3 and Fig. 2). Most stable

Table 1. Phase transition temperatures T_D and enthalpies ΔH obtained for compounds CM1, CM2 and mixture W1000 by combined method of DSC and texture observations under polarizing microscope

LC	SmC_A		SmC^*		SmA^*		Iso	
CM1	•	103.1	•	104.3	•	109.2	•	T_D [C deg]
		0.10		0.06		3.81		ΔH [kJ/mole]
CM2	•	85.67	•	100.2	•	101.7	•	T_D [C deg]
		0.01		0.10		7.72		ΔH [kJ/mole]
W1000	•	99.2	•	101.5	•	103.5	•	T_D [C deg]
		0.08		1.00		3.41		ΔH [kJ/mole]

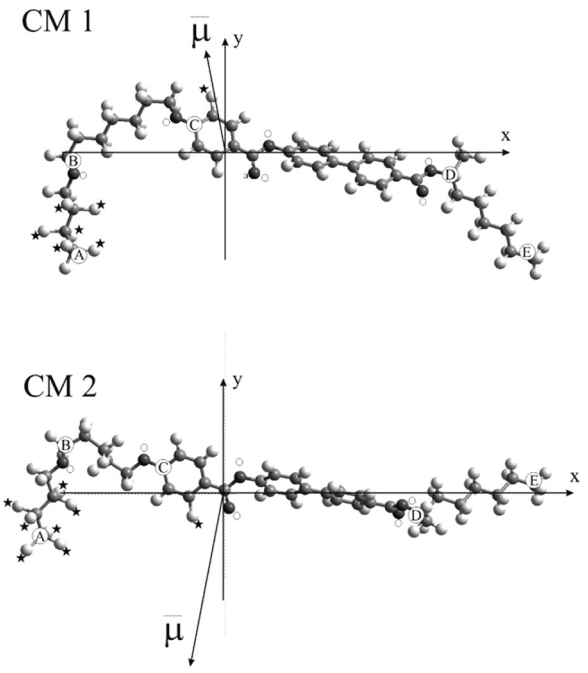

Figure 2. The projection of the calculated most stable molecular conformations of CM1 and CM2 compounds at the molecular energy minima on the Oxy plane. Ox axis is collinear with the molecular main axis of inertia. Oy axis is collinear with the minor axis of inertia. $\bar{\mu}$ denotes the projection of the molecular dipole moment on Oxy plane. Fluorine atoms are marked with stars. Oxygen atoms are marked with open circles. The molecular length for an elongated molecular conformation L_{max} was calculated as the distance between A – B – C – D – E carbon atoms. The end-to-end molecular length at most stable conformation was calculated as a distance between carbon atoms A and E.

molecular conformation was found for the single molecule (at the gaseous state) at the global molecular energy minimum. For both molecules a single molecular conformation characterized by the deep global minimum of energy was found.

Table 2. Molecular parameters and the tilt angle obtained from molecular modeling, structural and optical investigations. L_{max} – molecular length of the most extended molecular conformation, L – end-to-end molecular length (A-E distance, see Fig. 2), d_A – the layer spacing at T_c, d_{CA} – the saturated layer thickness at $T - T_c = -70$[K], θ^A_{opt} the tilt angle at T_c obtained by optical method, θ^{CA}_{opt} the saturated tilt angle at $T - T_c = -70$[K] obtained by optical method, θ^{CA}_{XRD} – the tilt angle calculated using Eq. (3), L^{CA}_{calc} – the molecule/dimer length calculated according to Eq. (4) and $d_x = d_{CA}$ and $\theta_{opt} = \theta^{CA}_{opt}$

	L_{max} [Å]	L [Å]	d_A [Å]	d_{CA} [Å]	θ^A_{opt}	θ^{CA}_{opt}	θ^A_{deV} (L)	θ^A_{deV} (L_{max})	θ^{CA}_{XRD} (L_{max})	L^{CA}_{calc} [Å]
CM1	40.2	30.0	30.9	29.2	0	38	0	39.8	43.5	37.1
CM2	37.2	31.9	33.7	33.6	32	43	–	25.1	25.4	45.9
W1000	–	–	34.4	31.2	31	42	–	–	–	42.1

Table 3. Results of the molecular modeling. The dipole moment calculations for compounds CM1 and CM2: μ_x, μ_y, μ_z – the x, y, z components of the molecular dipole moment, μ – the magnitude of the molecular dipole moment, $\mu_\perp$ – the component of the molecular dipole moment perpendicular to the molecular main axis of inertia, β – the angle between the molecular rigid core and the kinked part of the molecule given as the A-C-D angle (see Fig. 2)

		Dipole moment and dipole moment components [D]				
	β [°]	μ_x	μ_y	μ_z	μ	$\mu_\perp$
CM1	113.6	−1.39	7.26	−5.25	9.08	8.97
CM2	132.2	−1.96	−3.35	−5.25	4.97	4.57

The semi-empirical MNDO method [19] with Polak-Riberie algorithm of molecular modeling was applied. Subsequently results obtained from the MNDO method were tested and compared using force-field MM+ and Amber methods. Frames of coordinates were equally oriented for both considered molecules. The Ox axis was oriented along the molecular main axis of inertia, the Oy axis was along the minor axis of inertia (see Fig. 2). The molecular length for the most elongated molecular conformation L_{max} was calculated as A – B – C – D – E distances (see Fig. 2). The end-to-end molecular length L was calculated as a distance between carbon atoms A and E. Results of these calculations are presented in Table 2 and in Figure 2.

The helical pitch was studied by combined method: the selective reflection method [20] and the direct observations of so called dechiralization lines [21,22]. As far as the selective reflection method is concerned the Shimazu UV-3600 Spectrophotometer with measuring range of 360–3000 [nm] was used. Tested compounds were placed on glass substrates and heated to the isotropic state. Top surface of each substrate glass was covered by silane coupling agent which together with the action of the free surface induced the homeotropic orientation of molecules within the whole sample. Studies were done upon slow cooling (0.1 [K/min]) from the orthogonal (SmA^*) phase through the synclinic (SmC^*) to the anticlinic (SmC^*_A) one. The cooling operation was done using a Peltier cell. Studies of the selective reflection of light for compounds under study were performed at transmission mode at the normal incidence. The helical pitch p of investigated compounds was calculated using selective reflection wavelength λ_{max} and well known formula $\lambda_{max} = \mathrm{p} \cdot n$ (thus $p = \lambda_{max}/n$). For all studied compounds the average refractive index $n = 1.5$ was taken [23]. For the W1000 mixture, at the low temperature range ($T < 95°C$) at SmC^*_A phase, the selective reflection was not observed in the measureable wavelength range, suggesting a long helical pitch.

For both CM1 and CM2 compounds at the SmC^*_A phase the detected selective reflection peak was weak and fuzzy. Due to this the helical pitch p of studied compounds at the SmC^*_A phase was additionally approximated from the periodicity of dechiralization lines. For this measurement several custom made cells were prepared. Cells thickness was stabilized by glass spacer of thickness $d = 50$ [μm]. The orienting layers were prepared by spincoating of the solution of Nylon 6/6 in 2,2,2-trifluoroethanol on substrate glasses which were subsequently dried, baked and rubbed. Cells were filled with the material under study at the isotropic state by the capillary

action. The planar, near bookshelf structure was formed upon a few cycles of slow heating/cooling cycles through SmA*-SmC* phase transition at the vicinity of the low frequency electric field (i.e., U = 160 [V], f = 15 [Hz]) and at the temperature gradient of 0.03 [K/min]. The observation of dechiralization lines was done upon continuous slow cooling from SmA* phase with the temperature gradient of 0.1 [K/min]. Using this method a repetitive results were obtained for the W1000 mixture only. The thermal behavior of the helical pitch vs. reduced temperature obtained by combined method for all studied mesogens, are presented in Figure 3.

The electrooptical response of mesogens under study was tested using SSAFLC structure obtained in thin standard cells (the cell gap was about 1.5 [μm]). The anti-parallel rubbing was applied for both boundary surfaces of cells. Cells were filled by the capillary action with compounds under study at the isotropic state. The uniform quasi-bookshelf structures were obtained during several slow melting-cooling cycles at the temperature gradient of 0.05 [K/min], in the presence of the electric field (E = 12 [V/mm], f = 15 [Hz], triangle pulse).

The tilt angle was measured using cells described above and electrooptical method presented elsewhere [24,25]. The results of the tilt angle measurement are presented in Figure 4.

The same cells were used for investigations of the spontaneous polarization P_s and rotational viscosity γ of single compounds and their bicomponent mixture W1000. The rotational viscosity γ was evaluated from the measurements of the switching time ON (τ_{10-90}) [26] upon square driving pulse at saturated voltage, using practical formula [27]:

$$\gamma = \frac{1}{1.8} P_S E \tau_{10-90} \tag{1}$$

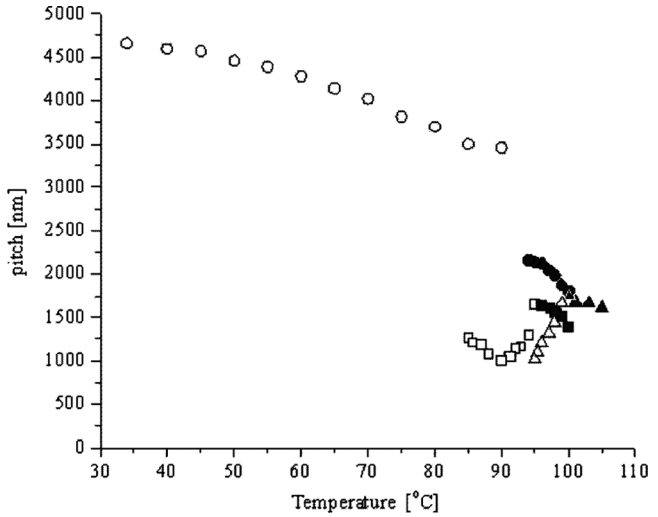

Figure 3. The helical pitch of single compounds CM1 (squares: □ and ■) are, CM2 (triangles: Δ and ▲) as well as for the bicomponent mixture W1000 (circles: o and ●) obtained by combined methods. Open figures are for the SmC^*_A phase, full figures are for synclinic the SmC* phase.

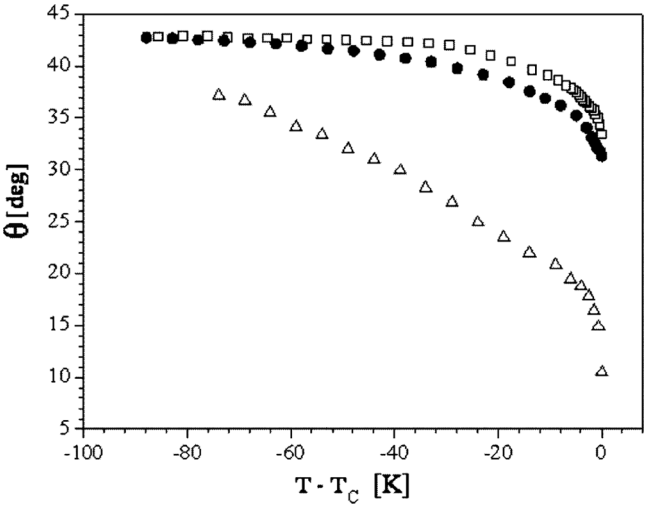

Figure 4. The tilt angle vs. reduced temperature for compounds CM1 (triangles Δ), CM2 (squares □) and their bicomponent mixture W1000 (circles ●) obtained by optical switching method.

where

$$E = \frac{U}{d}. \tag{2}$$

U denotes the applied voltage, d stands for the cell gap. The Arrhenius plot is presented in Figure 5. The spontaneous polarization P_s was evaluated from the

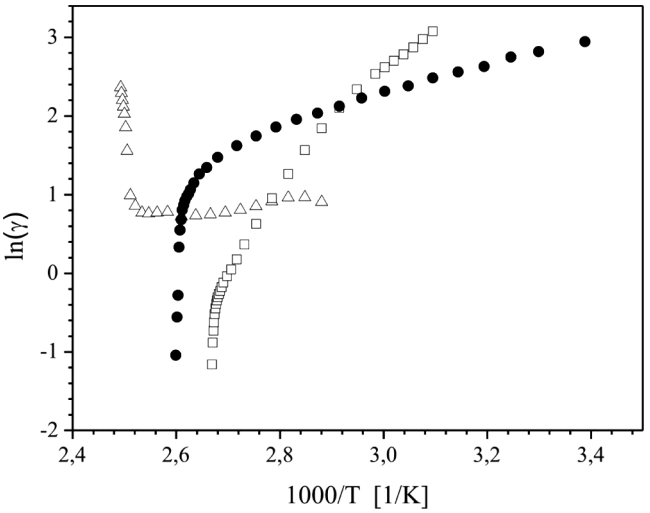

Figure 5. The Arhenius plot of lnγ vs. 1000/T [1/K] for compounds CM1 (triangles Δ), CM2 (squares □) and their bicomponent mixture W1000 (circles ●).

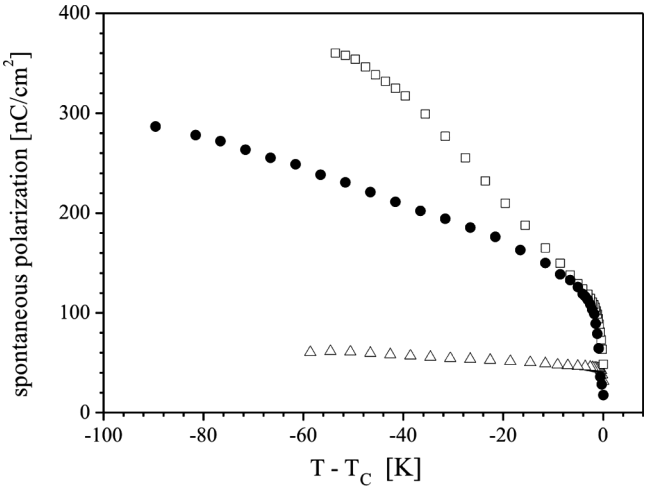

Figure 6. The spontaneous polarization of compounds CM1 (triangles Δ) and CM2 (squares □) and their equimolar bicomponent mixture W1000 (circles ●) vs. reduced temperature.

integration of the depolarization current peaks under triangle electric pulse. The results of the spontaneous polarization P_s measurements are presented in Figure 6.

The variation of the smectic layer thickness was measured by using of a Bruker D8 Discover XRD system equipped with Anton Paar DCS350 heating stage. Compound under study was placed into a thin wall capillary which was mounted within a heating stage in the path X-ray beam ($Cu_{K\alpha}$ line) path. The sample was initially heated to the isotropic state and subsequently slowly (the temperature gradient was 1 [K/min]) cooled to the temperature of a single measurement. During measurements the temperature stability was better than 0.1 [K]. Results of these studies are presented in Figure 7.

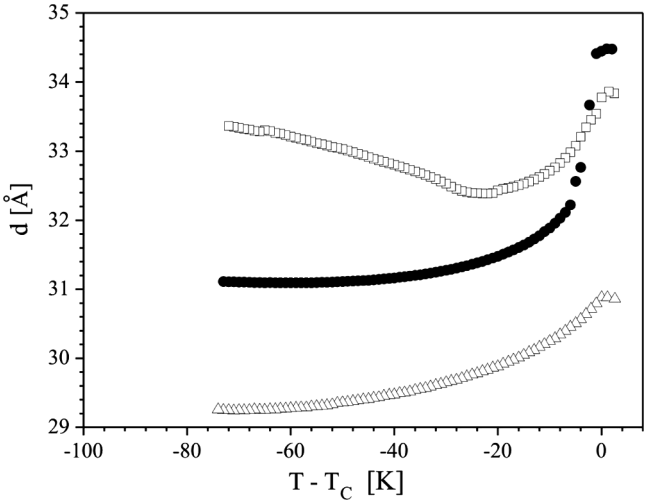

Figure 7. The layer spacing for compounds CM1 (triangles Δ), CM2 (squares □) and their bicomponent mixture W1000 (circles ●) obtained by XRD method.

Results and Discussion

The mesogenic behavior of the bicomponent mixture W1000 reveals that expected wide temperature range of the SmC^*_A phase was successfully achieved. The orthogonal SmA^* phase is preserved what is important for induction of the optically uniform surface stabilized bookshelf structure within the measuring cell. The DSC studies prove, that the W1000 mixture does not exhibit overcooled phase transition, what was observed for single compounds CM1 and CM2 (see Fig. 1). The synclinic SmC^* phase observed for single compounds CM1 and CM2 is almost suppressed by anticlinic SmC^*_A one for of the mixture W1000.

It is worth noting that the enthalpy of the phase transition from the orthogonal SmA^* phase to synclinic SmC^* one for the mixture W1000 is approximately one order of magnitude bigger than those for pure compounds CM1 and CM2. This is accompanied by the remarkable change of the layer spacing and the tilt angle temperature dependences. This could be explained by the dramatic change of the intralayer molecular arrangement of molecules at smectic phase of the mixture W1000 in comparison with pure compounds CM1 and CM2. Let us consider separately compounds CM1, CM2 and their equimolar mixture W1000.

Ad. CM1

Comparing the end-to-end molecular length $L = 30.0$ [Å] of the CM1 compound (see Table 2 and Fig. 2) with the layer thickness $d_A = 30.6$ [Å] at the SmA^*-SmC^* phase transition one can see that those values are near equal (see Fig. 7). The observation of the layer spacing d_A suggests that molecules adopt largely hockey stick like conformation presented in Figure 2. This implies the standard model of the SmA^* phase where molecules are (on average) orthogonal to the smectic later surface. However, if we consider the layer spacing d_{CA} at the SmC^*_A phase (see Table 2), one can see the difference between the saturated tilt angle measured for this phase by optical method $\theta^{CA}_{opt} = 38^\circ$ and the tilt $\theta^{CA}_{XRD} = 43.5^\circ$ calculated from Eq. (3):

$$\theta_{XRD}(L_x) = a\cos\left(\frac{d_x}{L_x}\right), \tag{3}$$

where $d_x = d_{CA}$, $L_x = L_{max}$. The value of θ^{CA}_{XRD} would equal θ^{CA}_{opt} under assumption of the existence of the phase with the dimers [28,29] consisting of two antiparallel oriented molecules. Such anticlinic phases were suggested earlier by us [30] as well as by Rieker and Janulis [31,32]. The average length of the molecular dimer $L^{CA}_{calc} = 37.1$ [Å] at the SmC^*_A phase was calculated according to formula (4):

$$L_{calc} = \frac{d_x}{\theta_{opt}} \tag{4}$$

where $d_x = d_{CA}$ and $\theta_{opt} = \theta^{CA}_{opt}$. This dimer is assumed to consists of molecules at hockey stick like conformation similar to this presented in Figure 2.

The further judgment of the interlayer interactions of compound CM1 can be drawn from investigations of the rotational viscosity. As one can see in Figure 5 the rotational viscosity of compound CM1 drops abruptly upon cooling through the SmA^*-SmC^* phase transition and saturates at the further cooling. This is in

contrary to typical behavior of the rotational viscosity of SmC* phases formed by homostructural compounds [26,30,33,34]. This supports the postulate given above, that at the SmA*-SmC* phase transition is accompanied by the dramatic change of the intralayer molecular arrangement and interactions (i.e., formation of the dimeric structure).

Ad. CM2

The layer spacing at the SmA* phase is $d_A = 33.7$ [°] (see Table 2). This value is close to the molecular end-to-end length L of the molecule at hockey stick like conformation (see Fig. 2). However, taking in to account the reasonable value of the tilt $\theta^A_{opt} = 32°$ at the temperature $T = T_c$ and the unsaturated characteristics of the layer spacing d vs. temperature T, the existence of the de'Vries-like SmA* phase can be postulated [28,30]. We assume that de'Vries-like SmA* phase is formed by the molecular dimers of average length $L^A_{calc} = 39.7$[Å] which was approximated according to formula (4) with $d_x = d_A$ and $\theta_{opt} = \theta^A_{opt}$.

The layer spacing of compound CM2 studied upon cooling though SmC* and SmC^*_A phases behaves irregular (see Fig. 7). It initially decreases to minimal value of $d = 32.3$ [Å] and subsequently increasing to the 33.4 [Å]. Such a change (approx. 3% only) of the layer spacing upon cooling through 70 [K] accompanied by the minor change of the tilt angle suggests the graduate changes of intralayer molecular arrangement.

Let us consider results of the layer spacing and the tilt angle of these phases. The saturated value of the tilt angle measured by the optical method is $\theta^{CA}_{opt} = 43.0°$ while the value of $\theta_{XRD}(L_{max})$ calculated using Eq. (3) is 25,4° only. As to satisfy the optical observations of the tilt angle $\theta^{CA}_{opt} = 43.0°$ the dimer length of $L^{CA}_{calc} = 45.9$ [Å] should be assumed. This is almost 9 [Å] more than L_{max}. This supports the postulate that the molecular dimer is build at the SmC^*_A phase of CM2 compound. The graduate evolution from the shorter dimer present in the SmA* phase to the longer one at SmC^*_A phase is postulated. It could explain the irregular behavior of the layer spacing at simultaneous regular and monotonous change of the tilt angle.

Ad. W1000

Among three studied smectogens the highest value of the layer spacing $d_A = 34.5$ [Å] is observed at the SmA* phase of the bicomponent mixture W1000. Such a space gap cannot be filled with molecules at most elongated molecules of length L_{max}. Hence, the existence of the de'Vries-like SmA* phase is assumed [30], This assumption is justified by the optical tilt observation at $T = T_c$, where $\theta^A_{opt} = 30°$. Moreover, a strong electroclinic effect is observed at SmA* phase, what is characteristic for de'Vries-like orthogonal phases. The layer spacing drops abruptly at the SmA*-SmC* phase transition and saturates at the value of $d_{CA} = 31.2$ [Å] at $T - T_c = -70$ [K]. This is accompanied by increase of the tilt angle by 12°. The saturated length of the molecular dimer $L^{CA}_{calc} = 42.1$ [Å] can be approximated according to Eq. (4).

The study of the spontaneous polarization confirm the great influence of the molecular intralayer interactions on the hindered molecular rotation. Compound CM1 exhibits the saturated value of the spontaneous polarization $P_s = 61$ [nC/cm^2] (see Fig. 6) at the value of the perpendicular component of the molecular dipole moment $\mu_\perp = 8.97$ [D]. This is a small part of the spontaneous polarization

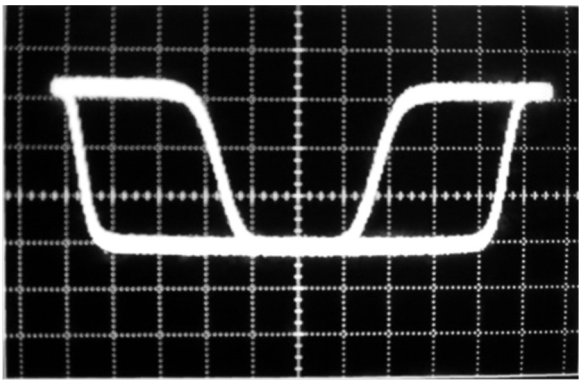

Figure 8. The oscillogram describing the electrooptical response of the W1000 mixture in the thin cell placed between crossed polarizers. The cell of thickness was 1.54 [μm]. The triangle pulse of 27 [V] peak-peak at frequency f = 100 [mHz] was applied. The threshold voltage is approximately 20 [V]. The saturation voltage for full switching is 25 [V].

$P_s = 362$ [nC/cm^2] exhibited by the homostructural compound CM2 with the molecular dipole moment $\mu_\perp = 4.57$ [D] only. This observation suggests that the long carboxylic spacer at the perfluorinated aliphatic chain hampers the molecular rotation [4,18,35] and supports dipole-dipole interactions inducing the dimeric intralayer molecular arrangement.

The successful induction of the long helical pitch at the low temperature SmC^*_A structure of the W1000 binary mixture is possibly obtained due to the diminishing of the interlayer interactions influenced by the chiral properties of molecules.

Since the temperature behavior of the helical pitch of CM1 and CM2 compounds seems to follow pictures previously observed [20,36–38], the pitch evolution of mixtures W1000 seems to be very intriguing.

For the first, thermal characteristics of helical pitch at the SmC^*-SmC^*_A phase transition, is discontinuous. For the second, it becomes longer upon the SmC^*-SmC^*_A phase transition and for the third, it continuously increases upon cooling. The saturated magnitude reaches value of 4700 [nm]. This value is enough for obtaining a helix free structure within the cell gap of 1.5 [μm]. Using this compound desired electrooptical performance, without any traces of the pretransitional effect was obtained (see Fig. 8) within the standard cell with cell gap of 1.5 [μm]. As one can see the full relaxation of the anticlinic state at the zero electric field is obtained.

Conclusions

The extraordinary long molecular pitch at the anticlinic SmC^*_A phase of the bicomponent mixture W1000 was successfully induced. The long pitch at SmC^*_A phase enables forming of a bookshelf structure with absolutely unwound helix. Such a structure exhibit electrooptical switching without traces of the pretransitional effect. The full relaxation of an anticlinic state is present at the zero electric field state. Due to this the near perfect dark state is observed (practically limited by the quality of used polarizers) despite the fact that the tilt angle is not the saturated 45° but 43°. On the basis of consideration presented here and similar results presented by us

earlier [30,34,39] for homostructural compounds one can collect some hints for long pitch OAFLC formulation:

1) Highly tilted anticlinic phases are easily formed when perfluorinated molecules posses the molecular dipole moment near perpendicular to the molecular main axis of inertia and hockey stick like conformation.
2) Such homostructural compounds can be mixed without dramatic influence on the mesogenic behavior. The temperature rage of the highly tilted anticlinic phase can be broaden, when compounds with low enthalpy phase transitions are added.
3) At the highly tilted anticlinic structure Molecular intralayer arrangement is usually dominated by molecular dimmers.
4) The helical pitch can be extended while dimers are formed by non equal molecules. At this case the chiral interlayer interactions can be diminished.
5) The rotational viscosity, the spontaneous polarization and tilt angle can be strongly affected be the intralayer molecular arrangement.
6) The influence of the spacer group within the lateral substituent on physical and structural properties is confirmed.

Acknowledgments

This work was supported from funds of Polish "MNiSW" for science at years 2008–2010 under grant KBN No. N N 507 445034 (PBG 12-427/2008 at WAT). The XRD analysis was kindly provided by dr Damian Pociecha of Warsaw University, Poland. Spectroscopic measurements were kindly performed by W. Rejmer from Institute of Chemistry, MUT, Kaliskiego 2 St. 00-908 Warszawa, Poland.

References

[1] D'have, K., Dahlgren, A., Rudquist, P., Lagerwall, J. P. F., Anderson, G., Matuszczyk, M., Lagerwall, S. T., Dąbrowski, R., & Drzewiński, W. (2000). *Ferroelectrics*, *244*, 115.
[2] D'have, K., Rudquist, P., Lagerwall, S. T., Pauwels, H., Drzewiński, W., Dąbrowski, R. (2000). *Applied Physics Letters*, *76*, 3528.
[3] Chandani, A. D. L., Górecka, E., Ouchi, Y., Takezoe, H., & Fukuda, A. (1989). *J. J. Appl. Phys.*, *28*, L1265.
[4] Dąbrowski, R., Gąsowska, J., Otón, J. M., Piecek, W., Przedmojski, J., & Tykarska, M. (2004). *Displays*, *25*, 9.
[5] Piecek, W., Raszewski, Z., Perkowski, P., Kedzierski, J., Rutkowska, J., Zielinski, J., Nowinowski-Kruszelnicki, E., Dabrowski, R., Tykarska, M., & Przedmojski, J. (2005). *Mol. Cryst. Liq. Cryst.*, *436*, 149/[1103].
[6] Czupryński, K., Gasowska, J., Tykarska, M., Kula, P., Soko, E., Piecek, W., Oton, J. M., & Castillo, M. P. L. (2005). *Journal of Optical Technology (A Translation of Opticheskii Zhurnal)*, *72*, 655.
[7] Lagerwall, S., Dahlgren, A., Jagemalm, P., Rudquist, P., D'Have, K., Pauwels, H., Dabrowski, R., & Drzewinski, W. (2001). *Adv. Func. Mat.*, *11*, 87.
[8] Yamada, Y., Yamamoto, N., Mori, K., Nakamura, K., Hagiwara, T., Suzuki, Y., Kawamura, I., Orihara, H., & Ishibashi, Y. (1990). *J. J. Appl. Phys., Part 1*, *29*, 1757.
[9] Mikułko, A., Marzec, M., Wrobel, S., & Dąbrowski, R. (2006). *Opto-Electr. Rev.*, *14*, 319.
[10] Zhang, S., Wen, B., Keast, S. S., Neubert, M. E., Taylor, P. L., & Rosenblatt, C. (2000). *Phys. Rev. Lett.*, *84*, 4140.
[11] Li, J.-F., Xin-Yi, W., Kangas, E., Taylor, P. L., & Rosenblatt, C. (1995). *Phys. Rev. B*, *53*, R13075.

[12] Beccherelli, R., & Elston, S. J. (1998). *Liq. Cryst.*, *25*, 573.
[13] Ikeda, S., Ogasawara, T., Nakata, M., Takanishi, Y., Ishikawa, K., & Takezoe, H. (2001). *Phys. Rev. E*, *63*, 061703.
[14] Gąsowska, J., Dabrowski, R., Drzewinski, W., Filipowicz, M., Przedmojshi, J., & Kenig, K. (2004). *Ferroelectrics*, *309*, 83.
[15] Żurowska, M. & Dabrowski, R. (2009). *Mol. Cryst. Liq. Cryst.*, in press.
[16] Żurowska, M., Dąbrowski, R., Dziaduszek, J., Czupryński, K., Skrzypek, K., & Filipowicz, M. (2008). *Mol. Cryst. Liq. Cryst*, *495*, 145.
[17] Rejmer, W., Żurowska, M., Dąbrowski, R., Raszewski, Z., & Piecek, W. (2009). *Mol. Cryst. Liq. Cryst*, *509*, 195[937].
[18] Żurowska, M., Dąbrowski, R., Dziaduszek, J., Czupryński, K., Skrzypek, K., Filipowicz, M., Bennis, N., & Otón, J. M. (2008). *Opto-Electr. Rev.*, *16*, 92.
[19] Dewar, M. J. S. & McKee, M. L. (1977). *J. Am. Chem. Soc.*, *99*, 4899.
[20] Li, J.-F., Takezoe, H., & Fukuda, A. (1991). *J. J. Appl. Phys.*, *30*, 532.
[21] Glogarova, M., Lejcek, L., Pavel, J., Janovec, V., & Fousek, J. (1983). *Mol. Cryst. Liq. Cryst.*, *91*, 309.
[22] Brunet, M., & Williams, C. (1978). *Ann. Phys.*, *3*, 237.
[23] Raszewski, Z., Kędzierski, J., Perkowsk, P., Piecek, W., Rutkowska, J., Kłosowicz, S., & Zieliński, J. (2002). *Ferroelectrics*, *276*, 289.
[24] Eidenschink, R., Geelhaar, T., Anderson, G., Dahlgren, A., Flatischer, K., Gouda, F., Lagerwall, S. T., & Skarp, K. (1988). *Ferroelectrics*, *84*, 167.
[25] Saipa, A. & Giesselmann, F. (2002). *Liq. Cryst.*, *29*, 347.
[26] Piecek, W., Rutkowska, J., Kedzierski, J., Perkowski, P., Raszewski, Z., & Dabrowski, R. (1997). In: *Proceedings of SPIE – The International Society for Optical Engineering*, *3318*, 148.
[27] Skarp, K. (1988). *Ferroelectrics*, *84*, 119.
[28] De Vries, A. (1979). *J. Chem. Phys.*, *71*, 25.
[29] Giesselmann, F., Zugenmaier, P., Dierking, I., Lagerwall, S. T., Stebler, B., Kaspar, M., Hamplová, V., & Glogarová, M. (1999). *Phys. Rev. E*, *60*, 598.
[30] Piecek, W., Raszewski, Z., Perkowski, P., Kędzierski, J., Rutkowska, J., Zieliński, J., Dąbrowski, R., & Sun, X. W. (2007). *Mol. Cryst. Liq. Cryst.*, *477*, 205[699].
[31] Rieker, T. P., & Janulis, E. P. (1994). *Liq. Cryst.*, *17*, 681.
[32] Rieker, T. P., & Janulis, E. P. (1995). *Phys. Rev. E.*, *52*, 2688.
[33] Piecek, W., Glab, K. L., Januszko, A., Perkowski, P., & Kaszynski, P. (2009). *J. Mat. Chem*, *19*, 1173.
[34] Piecek, W., Kula, P., Raszewski, Z., Perkowski, P., Morawiak, P., Kędzierski, J., Dąbrowski, R., & Sun, X. W. (2008). *Ferroelectrics*, *365*, 78.
[35] Raszewski, Z., Kędzierski, J., Perkowski, P., Rutkowska, J., Piecek, W., Zieliński, J., Żmija, J., & Dąbrowski, R. (1997). *Mol. Cryst. Liq. Cryst.*, *328*, 85.
[36] Lagerwall, J. P. F., Giesselmann, F., & Osipov, M. A. (2006). *Liq. Cryst.*, *33*, 625.
[37] Suwa, S.-I., Takanishi, Y., Hoshi, H., Ishikawa, K., & Takezoe, H. (2003). *Liq. Cryst.*, *30*, 499.
[38] Lagerwall, J. P. F. *et al.* (2000). *Ferroelectric Liquid Crystals*, Gordon & Breach: Germany.
[39] Piecek, W., Raszewski, Z., Perkowski, P., Przedmojski, J., Kedzierski, J., Drzewin ski, W., Dabrowski, R., & Zielinski, J. (2004). *Ferroelectrics*, *309–312*, [269]/125.